Continuous Polyolefin Cracking on an HZSM-5 Zeolite Catalyst in a Conical Spouted Bed Reactor

5 AUTHORS, INCLUDING:

Gorka Elordi
Universidad del País Vasco / Euskal Herriko …
33 PUBLICATIONS **725** CITATIONS

SEE PROFILE

Martin Olazar
Universidad del País Vasco / Euskal Herriko …
275 PUBLICATIONS **5,702** CITATIONS

SEE PROFILE

Gartzen Lopez
Universidad del País Vasco / Euskal Herriko …
81 PUBLICATIONS **1,456** CITATIONS

SEE PROFILE

Maite Artetxe
Universidad del País Vasco / Euskal Herriko …
29 PUBLICATIONS **531** CITATIONS

SEE PROFILE

Continuous Polyolefin Cracking on an HZSM-5 Zeolite Catalyst in a Conical Spouted Bed Reactor

Gorka Elordi,* Martin Olazar, Gartzen Lopez, Maite Artetxe, and Javier Bilbao

Department of Chemical Engineering (Group of Catalytic Processes and Residue Valorization), University of the Basque Country, P. O. Box 644, E48080 Bilbao, Spain

ABSTRACT: The effect of operating conditions on product yields and compositions has been studied in the catalytic cracking of polyolefins (high- and low-density polyethylene and polypropylene) in a conical spouted bed reactor. The catalyst has been prepared by agglomerating an HZSM-5 zeolite (SiO_2/Al_2O_3 = 30) with bentonite and alumina. The study has been carried out in continuous mode, in the 450−570 °C range, with polyolefin flow rates between 1 and 2 g min^{-1} and feeding up to 1 kg of polyolefin into a 30 g catalyst bed. The result is an excellent performance of the reactor−catalyst pairing for continuous catalytic pyrolysis, given that the yields obtained in the pyrolysis of high-density polyethylene at 500 °C without defluidization problems and very low catalyst deactivation are as follows: 60 wt % C_2−C_4 olefins, 15 wt % nonaromatic C_5−C_{11} hydrocarbons, 10 wt % single-ring aromatics, and 14 wt % C_{4-} alkanes. Only small differences are observed in the pyrolysis of the different polyolefins.

1. INTRODUCTION

The pyrolysis (thermal cracking) of waste plastics is an interesting route for the large-scale production of fuels and monomer recovery.[1−3] Different laboratory- or pilot-scale reactors have been studied: batch,[4−6] semibatch (with volatile removal),[7,8] fixed bed,[9] mechanically actuated conveyors (or screw kilns),[10,11] fluidized beds,[12,13] and conical spouted beds (CSBR).[14,15] The main difficulties that limit the larger scale implementation of the process are related to the sticky nature of the fused plastic, especially of polyolefins, and to the limitations of heat and mass transfer between phases.

The fluidized bed reactor performs well in terms of heat and mass transfer. Nevertheless, the conical spouted bed reactor allows for minimizing the serious problem of defluidization caused by a very sticky reaction medium, being especially suitable for reducing bed segregation when materials of different size and/or density are handled.[16,17] This allows for operating with the catalyst in situ without segregation problems. Furthermore, some of the difficulties involved in the scaling-up of this technology have been solved by using internal devices to control gas and solid flows.[18] In addition, the residence time of the volatiles is low (centiseconds),[19] which is suitable for a high yield of light olefins by minimizing their transformation into secondary products, such as methane, aromatics, and coke.[20,21] Elordi et al.[22] have operated with a continuous feed of high-density polyethylene (HDPE), and they emphasize the rapid and uniform coating of sand particles with fused plastic in a CSBR.

Moreover, the use of acid catalysts in situ allows for decreasing pyrolysis temperature (essential for the viability of a highly endothermic process) and increasing selectivity to products of high interest, as are olefins (raw material with an increasing demand) in the pyrolysis of polyolefins. Catalysts prepared on the basis of different zeolites (HY, HZSM-5, Hβ, and MCM-41) have been studied,[23−30] given that they activate the mechanism of carbocationic cracking of primary products from the thermal cracking of polyolefins (mainly waxes) and the subsequent reactions of isomerization, oligomerization−cracking, and hydrogen transfer.[31]

The main limitation on the use of catalysts is their deactivation by coke. Elordi et al.[32] studied the effect of the porous structure on the deactivation of catalysts prepared on the basis of HZSM-5, HY, and Hβ zeolites used in the pyrolysis of HDPE. The lower deactivation of the HZSM-5 zeolite is explained mainly by its tridimensional porous structure, which enhances the circulation of monoaromatic coke precursors toward the outside of the zeolite crystalline channels. A fact contributing to limiting coke deactivation is the generation of mesopores and macropores on the outside of the zeolite crystals by their agglomeration into a matrix of bentonite and alumina.[33] Furthermore, the high gas flow rate in the spouted bed reactor enhances the dragging of coke precursors within HZSM-5 crystals which, in addition to reducing the residence time, contributes to avoiding the formation of polyaromatics. This good performance of the HZSM-5 zeolite in attenuating coke deactivation is well-known in catalytic processes and, particularly, in the cracking of hydrocarbons and is explained in the literature on the basis of the nature and moderate strength of the acid sites and on pore size and microporous structure.[34−36]

This paper addresses key aspects in the continuous pyrolysis of polyolefins in a conical spouted bed reactor and determines the effect of reaction temperature, polyolefin flow rate, and polyolefin nature (low- and high-density polyethylene and polypropylene) on product yields and properties.

2. EXPERIMENTAL SECTION

2.1. Polyolefins Studied. The polyolefins (high-density polyethylene, HDPE; low-density polyethylene, LDPE; and

Table 1. Properties of the Polyolefins Used

material	M_w (g mol^{-1})	polydispersity	ρ (kg m^{-3})	HHV (MJ kg^{-1})
HDPE	46 200	2.89	940	43
LDPE	92 200	5.13	923	43
PP	50 000−90 000	2.00	890	44

polypropylene, PP) have been supplied by Dow Chemical (Tarragona, Spain) in the form of chippings (4 mm), and they have the properties set out in Table 1. The average molecular weight, M_w, polydispersity (ratio between the weight-average molecular weight and the number-average molecular weight), and density, ρ, have been provided by the supplier. The higher heating value has been determined by differential scanning calorimetry (Setaram TG-DSC 111) and isoperibolic bomb calorimetry (Parr 1356).

2.2. Equipment and Pyrolysis Conditions. The pyrolysis pilot plant has been described elsewhere.[20−22] The system for feeding polyolefins (in the form of chippings) involves a hopper (2 L) with an eccentric vibrator and a three-way hollow ball valve connected to a half-inch pipe cooled by tap water. The device is controlled by an automaton that programs the frequency for a Swagelok pneumatic actuator. Although the capacity of the original hollow ball valve corresponded to 0.4 g of polyolefin, the ball has been filled with silicone to reduce its capacity to 0.125 g of polymer, which is fed into the reactor every 7.5 s (8 batches min^{-1}) for a total feed of 1 g min^{-1}. The pipe for feeding polyolefin into the reactor is located over the fountain zone of the spouted bed in order to facilitate the fusion and the coating steps of the catalyst particles, which take place prior to cracking. Experimental operation has shown that this positioning of the inlet pipe has no influence on the results, as particles describe a cyclic movement with an average cycle time of around 1 s.

Furthermore, the influence of polyolefin fusion and catalyst particle coating on heat and mass transfer has been determined by carrying out blank assays without sand, catalyst, and inert gas. These experiments, consisting of polyolefin particles crossing the hot reactor from top to bottom (free fall condition), have revealed that the yield of volatiles is insignificant at the highest temperature studied (570 °C).

The spouted bed reactor, 3 L in volume, is of a conical shape with a cylindrical section in the upper part for the development of the fountain (Figure 1). The total height of the reactor, H_T, is 34.00 cm, with a conical section height, H_c, of 20.05 cm and a conical zone angle, γ, of 28°. The diameter of the cylindrical section, D_c, is 12.30 cm, the diameter of the base, D_i, is 2.00 cm, and that of the gas inlet, D_o, is 1.00 cm. These dimensions guarantee bed stability in a wide range of process conditions, and they have been established in previous hydrodynamic studies of conical spouted beds for different materials.[37−45] The N$_2$ flow rate is 11 NCL (Normal Condition Litres) min^{-1} measured at 450 °C, 1.2 times of that corresponding to the minimum spouting velocity for catalyst particles of a size between 0.6 and 1.2 mm. For a constant mass flow rate, an increase in temperature causes an increase in volume flow rate, which ensures that the velocity is higher than that corresponding to the minimum of spouting and, at the same time, shortens volatile residence time. Nevertheless, because the average residence time is very short, the effect of temperature is the only influential parameter in fast pyrolysis.

Two thermocouples are located inside the reactor, one in the bed annulus and the other one close to the wall. The reactor also
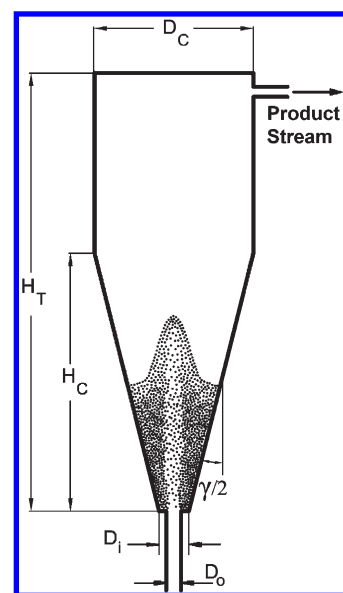

Figure 1. Diagrammatic representation of the reactor.

has a pressure gauge for measuring the total and differential pressure, which allows for detecting any increase in pressure drop due to the plugging of gas filters and thus leading to their substitution. In the reactor lid, and near the outlet for the volatile stream, there is an inlet for cyclohexane, which is fed as an inert standard compound to close the mass balance together with the results of the gas chromatograph. The outlet pipe for the volatile stream is located perpendicular to the reactor axis.

The condensation system for the volatile stream consists of the following: (i) a stainless-steel condenser cooled by an antifreeze mixture, which allows for lowering the temperature to −10 °C; (ii) two coalescence filters (made of epoxy ester), which retain over 99.5% of aerosol particles larger than 0.1 μm.

2.3. Product Analysis. The online analysis of the outlet volatile stream (very diluted in N$_2$) has been carried out by periodically sending samples to a gas chromatograph (Agilent 6890) equipped with a flame ionization detector (FID). The following temperature program has been used: (i) 4.5 min at 35 °C, for obtaining a good separation of C$_1$−C$_4$ hydrocarbons; (ii) a ramp of 15 °C min^{-1} up to 305 °C; and (iii) 5.5 min at 305 °C to ensure that all the hydrocarbons are eluted from the HP-PONA column. The yield of each compound has been calculated from the ratio between the corresponding chromatographic area and the sum of the areas for all of the compounds. The value of this ratio is multiplied by the yield of wax-free stream (one minus the yield of waxes calculated by weighing the waxes collected in the filters). Cyclohexane (0.1 mL min^{-1}) has been used as the internal standard to validate the mass balance.

A gas chromatograph/mass spectrometer (GC/MS; Agilent 3000 micro GC and Agilent 5975B inert MSD mass spectrometer) has been used to confirm the absence of hydrogen, carbon monoxide, and carbon dioxide, to determine the ethane/ethylene and propane/propylene ratios more accurately, and to identify the lightest components (with a molecular weight lower than 100 g mol^{-1}).

Identification of the liquid fraction components (obtained by condensation of the volatile fraction) and waxes (diluted in tetrahydrofuran at 55 °C) has been carried out by means of a gas chromatograph coupled with a mass spectrometer (Shimadzu

Table 2. Properties of the Catalyst

BET surface area ($m^2 g^{-1}$)	182	av pore diam (Å)	84
micropore ($d_p/Å < 20$) area ($m^2 g^{-1}$)	98	total acidity (μmol of NH_3 g^{-1})	142
mesopore ($20 < d_p/Å < 500$) vol ($cm^3 g^{-1}$)	0.26	av acid strength (kJ (mol of NH_3)$^{-1}$)	150
pore vol distribution (%)		acidity levels by TPD (%)	
$d_p/Å < 20$	4.5	$T/°C < 280$	34
$20 < d_p/Å < 500$	27.5	$280 < T/°C < 420$	52
$d_p/Å > 500$	68.0	$T/°C > 420$	14

QP2010S). A DB-1MS column of 60 m in length, 0.27 mm in inner diameter, and a thickness of 0.25 μm is used in the gas chromatograph. This column separates the products according to their molecular weight. The temperature sequence of the chromatograph oven has the following steps: (i) 40 °C for 2 min, (ii) a ramp of 4 °C min^{-1} up to 300 °C, and (iii) 300 °C for 6 min. The chromatographic analysis conditions are as follows: detected mass interval, 40–400; solvent delay, 4.5 min; injector pressure, 100.3 kPa; total flow rate, 93.2 mL min^{-1}; column flow rate, 0.89 mL min^{-1}; carrier gas linear velocity, 24.1 cm s^{-1}; split, 1000:1, although it has been reduced in certain cases to increase the peak resolution of the less abundant components.

2.4. Catalyst. A catalyst has been prepared on the basis of an HZSM-5 zeolite with a ratio of $SiO_2/Al_2O_3 = 30$, supplied by Zeolyst International (Kansas City, KS, USA). The HZSM-5 zeolite has been supplied in the ammonium form, so it has been calcined at 550 °C to obtain the acid form. To obtain particles with a suitable size (0.6–1.2 mm diameter range) and mechanical resistance for the conical spouted bed reactor, the zeolite particles (25 wt %) have been agglomerated by wet extrusion with bentonite (Exaloid; 30 wt %) and inert alumina (Martinswerk; 45 wt %). The agglomeration generates meso- and macropores in the particles, which have a positive effect on attenuating deactivation because they promote coke deposition on the outside of the pores and, consequently, minimize their external blockage.[33,46] Prior to use, the catalyst has been calcined at 575 °C for 2 h in a N_2 atmosphere. This temperature is suitable for eliminating the strong acid sites of the HZSM-5 zeolite by dehydroxylation, given that these sites are hydrothermally unstable.[47]

The physical properties (BET surface area, pore volume, and distribution; Table 2) are measured by N_2 adsorption–desorption (Micromeritics ASAP 2010). The macropore structure has been measured by means of Hg intrusion porosimetry (Micromeritics Autopore 9220). The HZSM-5 zeolite has a microporous structure involving two different types of elliptic channels (straight ones of 0.53 × 0.56 nm and sinusoidal ones of 0.51 × 0.55 nm), which bisect each other perpendicularly.[48,49] Table 2 also shows the values of total acidity and average acid strength. These results have been obtained by monitoring the differential adsorption of NH_3 simultaneously by calorimetry and thermogravimetry in a Setaram TG-DSC 111.[50] From the curves of the NH_3 temperature programmed desorption (TPD) determined by connecting a Balzers Instruments mass spectrometer (Thermostar) online to a Setaram TG-DSC 111, an acid site classification has been established according to the following desorption levels: weak acidity, 150–280 °C; average acidity, 280–420 °C; strong acidity, 420–550 °C (Table 2).

3. RESULTS

3.1. Effect of Reaction Temperature. Figure 2, where each graph corresponds to a given temperature in the 450–570 °C

range, shows the results of the evolution of product fraction yields with the polyolefin amount fed into the reactor: light olefins (C_2–C_4), light alkanes (C_{4-}), light liquid fraction (C_5–C_{11}, without aromatic components), single-ring aromatics, heavy liquid fraction (C_{12}–C_{20}), and waxes (C_{21+}). The results correspond to the transformation of HDPE, which is fed at a flow rate of 1 g min^{-1} into a bed of 30 g of catalyst.

The results in Figure 2 show the catalyst activity and its low deactivation in the whole temperature range. Only the runs of more than 5 h duration (over 300 g of HDPE fed into the reactor; Figure 2a, for 450 °C) show an incipient production of waxes (C_{21+}), which are thermal pyrolysis primary products that are transformed by the catalyst into lighter product fractions. This result is attributed to the fact that the process limiting step at 450 °C is the initial step of wax formation, which is extremely slow at this temperature. Consequently, the minimum temperature for thermal pyrolysis (without catalyst) is 500 °C.[22]

The yield of waxes (main product in thermal pyrolysis) is insignificant above 450 °C, which is evidence that the catalyst plays an essential role on product yields. Mastral et al.[12] used a fluidized bed reactor and also determined that complete conversion of HDPE is reached using an HZSM-5 catalyst above 450 °C. Nevertheless, operation is advisable above a minimum temperature of 500 °C in order to avoid the operational problems associated with the incipient formation of waxes in the reaction medium.

Figure 2b, corresponding to a long run (1 kg of HDPE fed into the reactor for 16.6 h) at 500 °C, shows that deactivation is low up to 400 g of HDPE fed into the reactor, with a minor decrease in the yield of C_2–C_4 olefins, with this yield and those of other product fractions subsequently remaining almost constant.

Figure 3 shows the effect of temperature on product fractions due to the effect of this variable on both the thermal cracking step of HDPE to form waxes and the catalytic cracking steps of these waxes. The latter catalytic cracking steps take place through a carbocationic mechanism, with secondary catalytic reactions of oligomerizaton–cracking, isomerization, and hydrogen transfer.[31] It is noteworthy that an increase in temperature gives way to a decrease in the yield of light olefins, from 57.8 wt % at 450 °C to 50.3 wt % at 570 °C, whereas the yield of single-ring aromatics increases, from 9.1 to 20.7 wt %, which is due to the enhancement of Diels–Alder condensation reactions.[51] A decrease is also observed in the yield of the nonaromatic C_5–C_{11} hydrocarbon fraction, from 16.6 wt % at 450 °C to 11.5 wt % at 570 °C. Nevertheless, there is no clear trend for the effect of temperature on the yields of light alkanes and the C_{12}–C_{20} fraction.

Regarding the gaseous product fraction, C_2–C_4 olefins are the main products (Figure 4) according to the following yield order: propylene > butenes > ethylene. As temperature is increased the yield of ethylene increases, but it is steady above 525 °C, around a

6063

dx.doi.org/10.1021/ie2002999 |*Ind. Eng. Chem. Res.* 2011, 50, 6061–6070
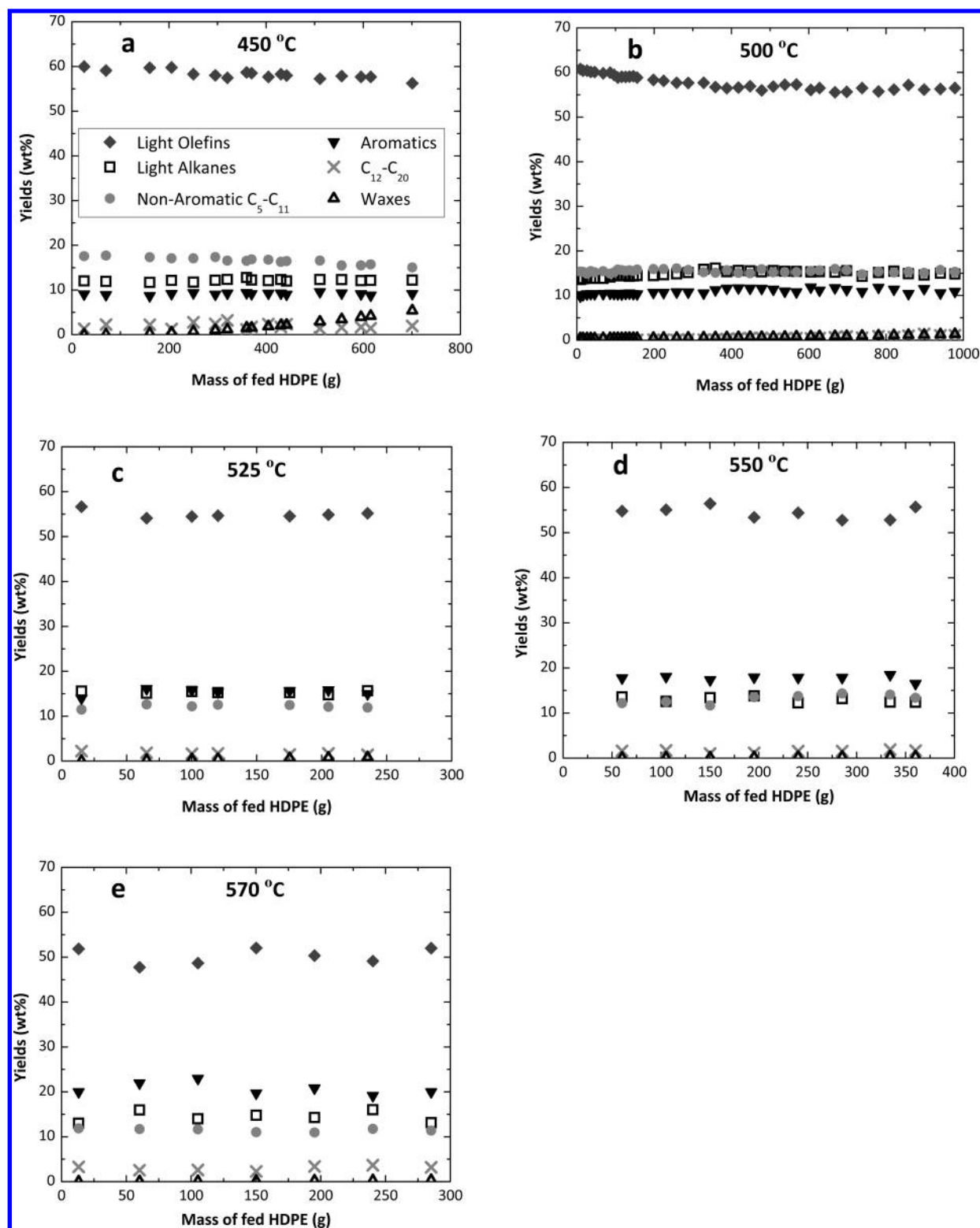
Figure 2. Evolution of product fraction yields with the amount of HDPE fed into the reactor for different temperatures: a, 450 °C; b, 500 °C; c, 525 °C; d, 550 °C; e, 570 °C.

value of 11.0 wt %. The yield of propylene peaks around 500 °C with a yield of 28.7 wt %. The yield of butenes decreases as temperature is increased and reaches a steady value of around 17.5 wt % above 525 °C. This re-distribution of olefins is due to the mechanisms of oligomerization−cracking that are characteristic of olefins when in contact with HZSM-5 zeolites, in which the selectivity to ethylene is enhanced as temperature is increased.[52,53]
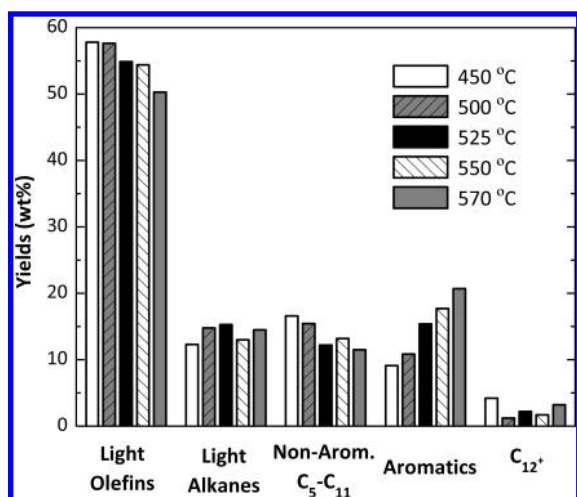
Figure 3. Effect of temperature on product fraction yields in the pyrolysis of HDPE.
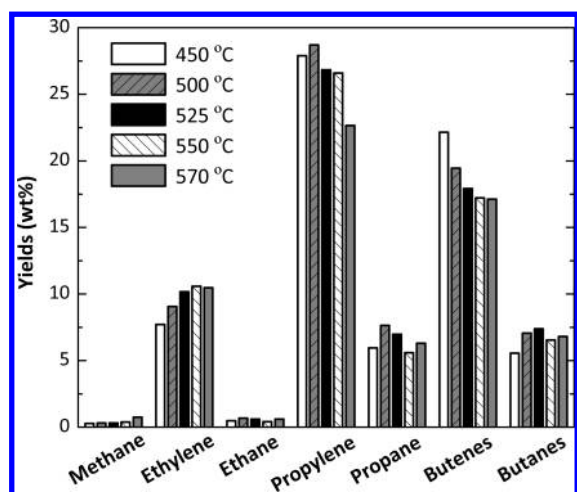

Figure 4. Effect of temperature on the yields of the gas fraction components in the pyrolysis of HDPE.

Figure 5. Effect of temperature on the yields of the C_5-C_{11} fraction components ordered according to the number of carbon atoms (a) and the type of bond (b), in the pyrolysis of HDPE.

The effect of temperature on the individual yields within C_2-C_4 paraffins is less significant, given that the formation of methane is significant only above 570 °C, with a yield of 0.8 wt %. The formation of methane is also observed at this temperature without a catalyst,[22] which is evidence that it is of thermal origin.

Figure 5 shows the effect of temperature on the yields of individual components in the gasoline fraction (made up of nonaromatic C_5-C_{11} hydrocarbon fractions and single-ring aromatics). The components of this fraction have been grouped according to the number of carbon atoms (Figure 5a) and types of bonds (Figure 5b). As the temperature is raised, the yield of C_5 components decreases, but increases in the cases of C_7, C_8, and C_9 (Figure 5a), which is explained by the olefinic nature of C_5 compounds and the aromatic character of C_7-C_9 compounds. This effect of temperature is explained by the cracking of C_{5+} olefins to form C_2-C_4 light olefins and the formation of aromatics by the condensation of C_2-C_4 olefins. Nevertheless, the aromatic components are not cracked under these conditions.[52]

The yield of C_6 components (including benzene) has recorded no significant change in the temperature range studied.
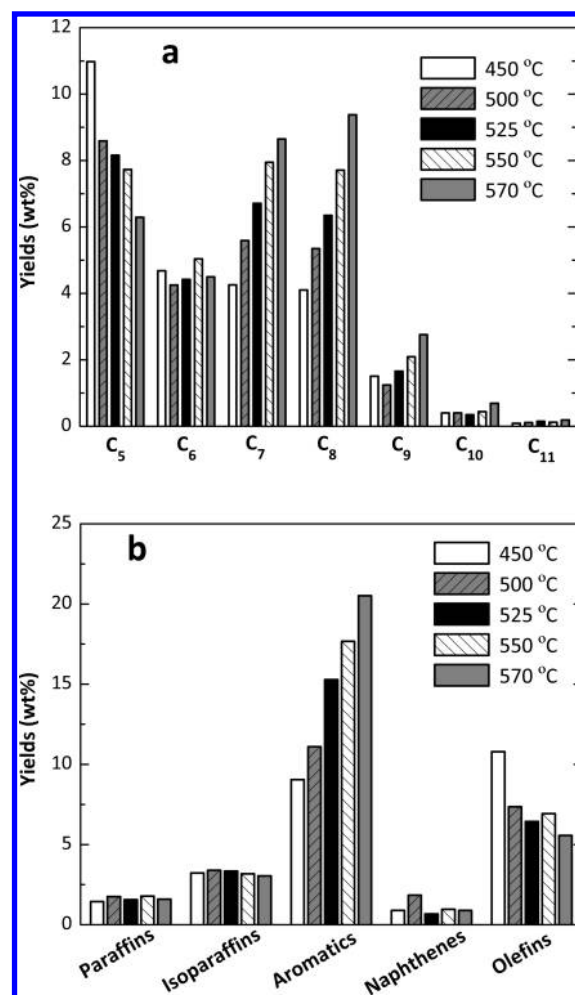
Likewise, there is no significant effect of temperature on the yields of paraffins, isoparaffins, and naphthenes in the C_5-C_{11} fraction, for which the reactions of conversion and formation seem to be balanced.

3.2. Effect of HDPE Flow Rate. The conical spouted bed reactor is highly versatile for operating in a wide range of bed voidages thanks to the versatility of the gas flow rate. By increasing gas velocity, operation can be carried out from the regime of the incipient spouted bed to the regime of the dilute spouted bed (jet spouted bed), through a transition regime in a wide range of gas velocities.[54] In the pyrolysis of polyolefins, the polyolefin flow rate may be increased almost indefinitely, as long as the mass of catalyst (or catalyst + sand) in the bed is increased in order to uniformly coat the solid particles with the fused plastic. The inert gas flow rate must also be increased in order to maintain the spouted bed regime. These changes impact the pyrolysis results.

Previous studies allow for establishing a minimum flow rate of 1 g min^{-1} of HDPE into a catalyst mass of 30 g to avoid fluctuations in the reaction medium concentration with time. The influence of increasing flow rate has subsequently been studied for the same amount of catalyst and, consequently, for the same gas flow rate. This means that the flow rate is increased
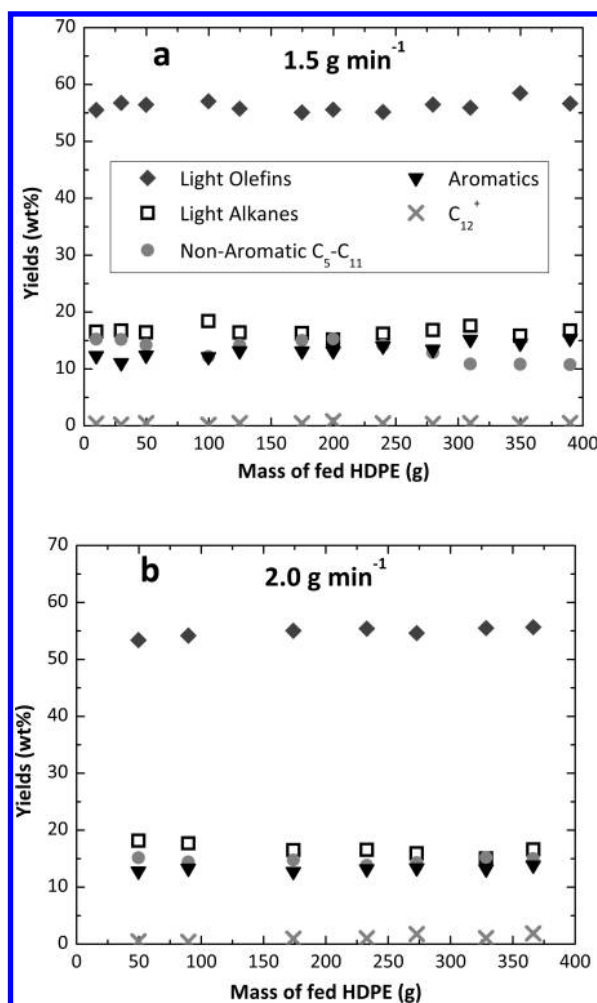
6065

dx.doi.org/10.1021/ie2002999 |*Ind. Eng. Chem. Res.* 2011, 50, 6061–6070

Figure 6. Evolution of product fraction yields with the amount of HDPE fed into the reactor for different flow rates of HDPE at 500 °C: a, 1.5 g min^{-1}; b, 2.0 g min^{-1}.
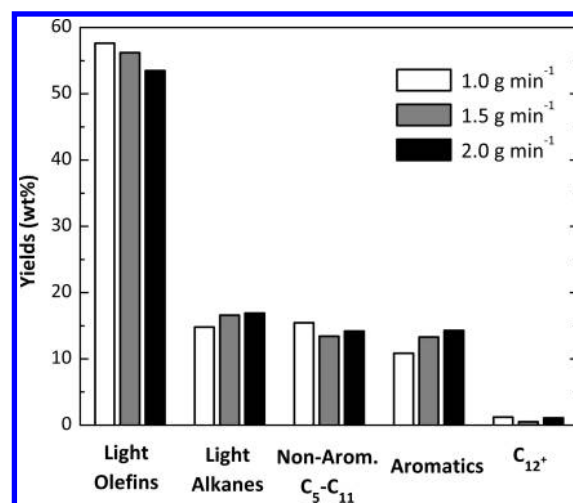

Figure 7. Effect of HDPE flow rate on product fraction yields at 500 °C.
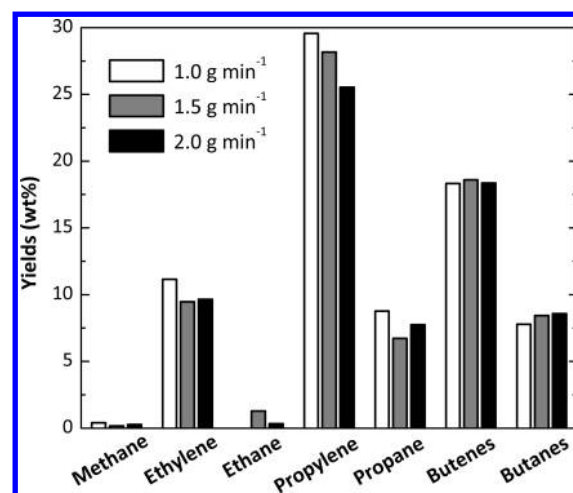
Figure 8. Effect of HDPE flow rate on the yields of the gas fraction components at 500 °C.

under the same hydrodynamic conditions in the bed (bed voidage, residence time of the volatiles, and so on), which allows for ascertaining the capacity for coating the catalyst particles with fused plastic. Furthermore, as the flow rate of HDPE is increased, the concentration of volatiles in the reaction medium also increases, which presumably enhances not only the reactions for transforming primary products (waxes) but also secondary reactions.

Figure 6 shows the evolution of product fraction yields at 500 °C with the flow rate of HDPE fed into the reactor. The results in Figure 6a correspond to a flow rate of 1.5 g min^{-1}, and those in Figure 6b correspond to 2.0 g min^{-1}. Given the low yield of the heaviest fractions, $C_{12}-C_{20}$, and the waxes (C_{21+}), they have been grouped into a fraction called C_{12+}. The results show the aforementioned versatility of the spouted bed reactor; i.e., there are small differences in the yields as the flow rate of HDPE is increased and the transformation into light products is completed thanks to the efficient coating of catalyst particles with the fused plastic.

The differences in the yields (Figure 7) are attributed to the increase in the concentration of volatiles in the reaction medium, which is around 3 wt % for the flow rate of 1 g min^{-1} and around 6 wt % for 2 g min^{-1}. When the flow rate of HDPE is increased,

the yield of C_2-C_4 olefins decreases slightly (from 58 wt % for 1.0 g min^{-1} to 54 wt % for 2.0 g min^{-1}) and the yields of single-ring aromatics and alkanes increase, because the increase in the concentration of volatiles in the reaction medium enhances both the reactions of condensation of C_2-C_4 olefins to form aromatics and the hydrogen-transfer reactions to form C_2-C_4 paraffins. The decrease in the yield of C_2-C_4 olefins mainly affects propylene and, to a lesser extent, ethylene, whereas the yield of butenes increases (Figure 8).

Figure 9 shows the effect of HDPE flow rate in the feed on the components of the gasoline fraction (including the fractions of nonaromatic C_5-C_{11} hydrocarbons and single-ring aromatics). It is observed that an increase in the flow rate of HDPE gives way to an increase in the yields of all of the compounds grouped according to the number of carbon atoms (Figure 9a). This is due to the increase in the yields of the aromatic, olefinic, and isoparaffinic components (Figure 9b), caused by the increase in the concentration of volatiles in the medium and their enhanced condensation and oligomerization of light olefins and the isomerization of paraffins.
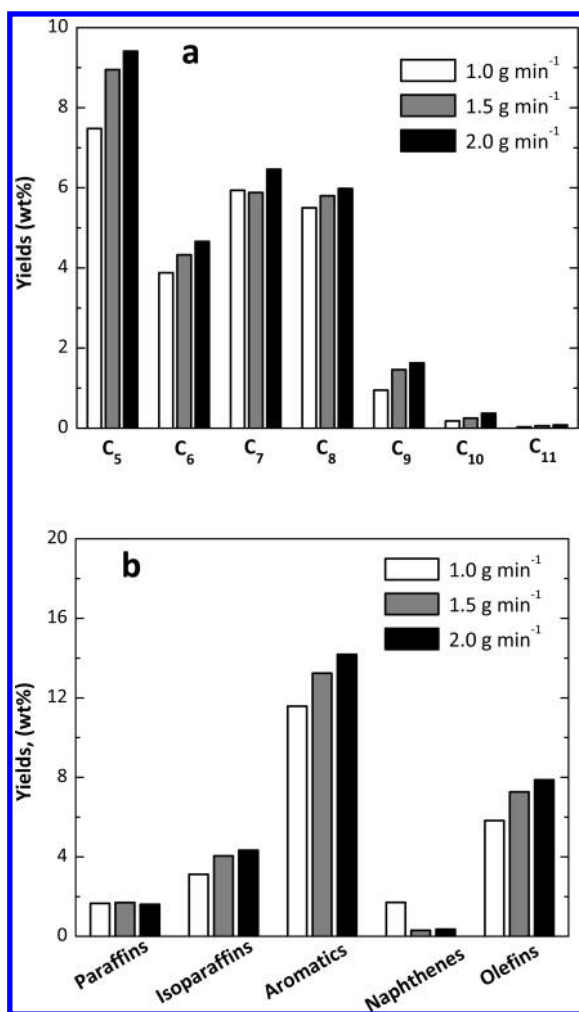
Figure 9. Effect of HDPE flow rate on the yields of the C_5-C_{11} fraction components, ordered according to the number of carbon atoms (a) and the type of bond (b), at 500 °C.

3.3. Effect of Polyolefin Type.

Figure 10 shows the evolution of product fraction yields for the pyrolysis of LDPE (a) and PP (b). It should be noted that a feed of LDPE involves more problems than one of PP due to its lower glass transition temperature.[55] The pyrolysis of PP (Figure 10b) has been studied for more than 25 h (more than 1500 g of PP fed into the reactor) in order to compare catalyst deactivation with that corresponding to the pyrolysis of HDPE at the same temperature (500 °C; Figure 2b). The results for PP pyrolysis show that there is a significant change in the distribution of product yields due to catalyst deactivation. The yield of C_2-C_4 olefins peaks for an amount of around 800 g of PP fed into the reactor, whereas the yields of nonaromatic C_5-C_{11} hydrocarbons, single-ring aromatics, and C_{12+} increase steadily. The yield of C_2-C_4 alkanes decreases steadily.

This effect of deactivation on the distribution of products is characteristic of processes on HZSM-5 zeolites, such as the transformation of methanol and ethanol into hydrocarbons,[56,57] in which light olefins are reaction intermediates that are transformed into higher hydrocarbons or into paraffins by condensation and hydrogen-transfer reactions, and these are affected first by the deactivation of the HZSM-5 zeolite by coke deposition, which occurs selectively on the strong acid sites.
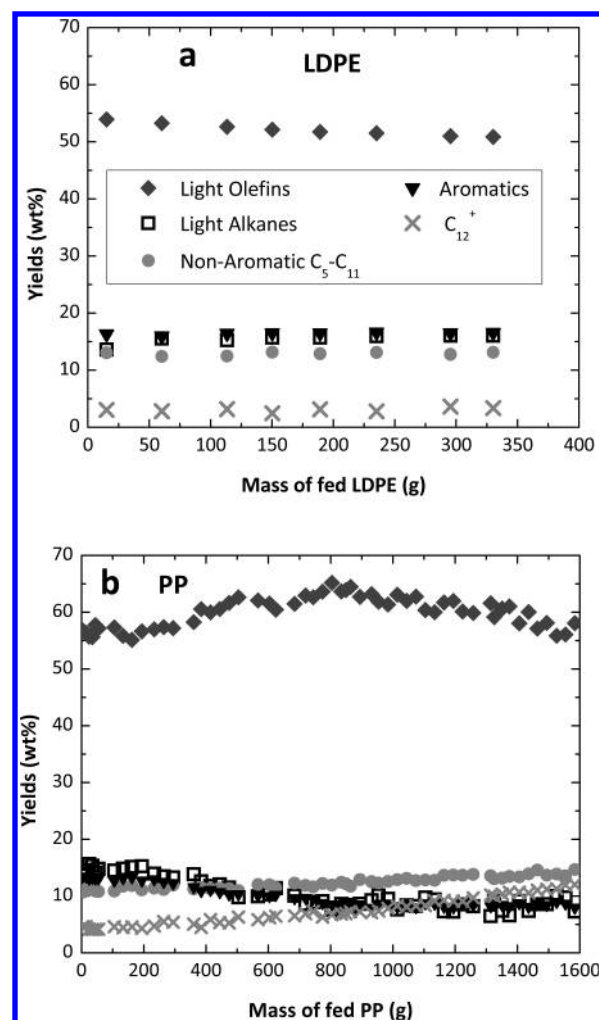

Figure 10. Evolution of product fraction yields with the amount of polyolefin fed into the reactor for different polyolefins at 500 °C: a, LDPE; b, PP.
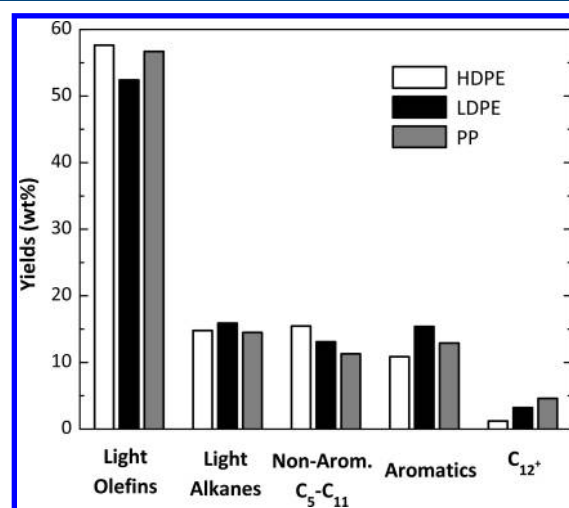

Figure 11. Comparison of product fraction yields in the pyrolysis of the three polyolefins at 500 °C.

Figure 11 compares the yields of the product fractions obtained with the three polyolefins and the fresh catalyst (zero
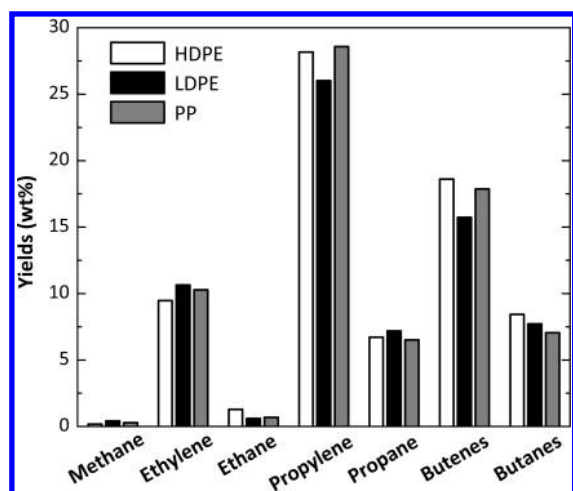
6067

dx.doi.org/10.1021/ie2002999 |*Ind. Eng. Chem. Res.* 2011, 50, 6061–6070

Figure 12. Comparison of gas fraction component yields in the pyrolysis of the three polyolefins at 500 °C.
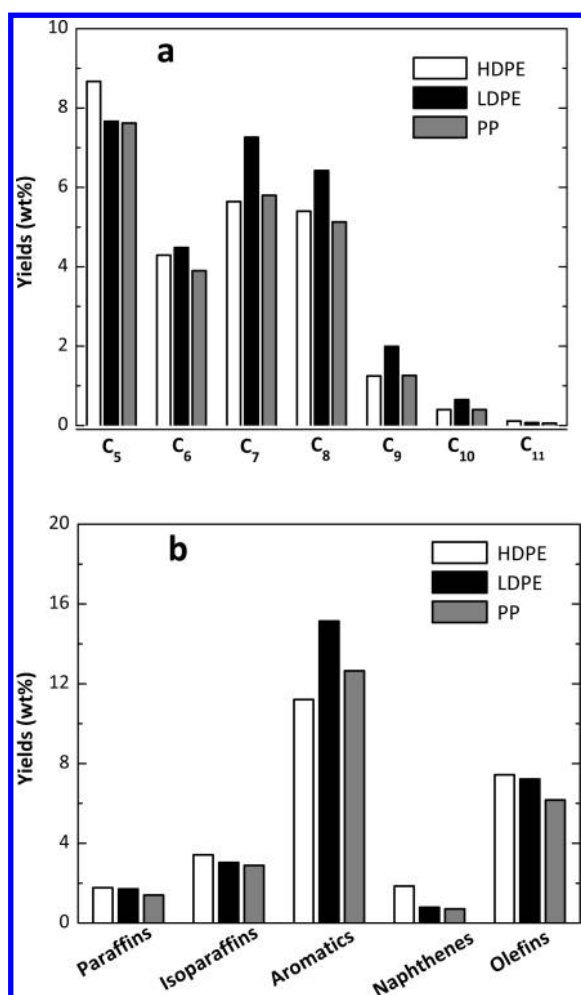

Figure 13. Comparison of the C_5-C_{11} fraction component yields in the pyrolysis of the three polyolefins at 500 °C, ordered according to the number of carbon atoms (a) and the type of bond (b).

time on stream). A lower yield of light olefins and a higher yield of light alkanes and aromatics are observed for LDPE. These differences are attributed to the shorter chains with a higher branching degree for LDPE, which makes its cracking easier and, consequently, facilitates a more rapid formation of olefins and their condensation steps to form aromatics or C_{12+} hydrocarbons. The higher yield of C_{12+} in the pyrolysis of PP is associated with the polymerizing capacity of propylene.

The similarity between the results for the different polyolefins is also observed by comparing the individual yields for the components in the gas fraction (Figure 12) and the yields in the gasoline fraction (C_5-C_{11} with aromatics), ordered according to the number of carbon atoms (Figure 13a) and to the bond type (Figure 13b). The lower yield of C_2-C_4 olefins in the pyrolysis of LDPE corresponds to a lower yield of propylene and butenes (Figure 12), and the higher yield of C_6-C_{10} fractions (Figure 13a) corresponds to the aforementioned higher yield of aromatic components in these fractions (Figure 13b).

It is difficult to compare the previous results with those obtained in the literature using different reactors and catalysts under different operating conditions, although they are consistent in that the differences between the yields for the different polyolefins are not significant in either thermal pyrolysis[58−62] or catalytic pyrolysis,[9,63] which ratifies the interest that pyrolysis has for a joint valorization of polyolefins, given that they account for approximately two-thirds of waste plastics.

4. CONCLUSIONS

The conical spouted bed reactor is suitable for the catalytic pyrolysis of polyolefins (HDPE, LDPE, and PP) in continuous mode for obtaining high yields of olefins and hydrocarbons of interest as fuel. The cyclic movement of the solid, characteristic of spouted beds, avoids the defluidization problems caused by the sticky nature of the solid. Furthermore, interesting facts to be noted are the quality of the coating of catalyst particles with the fused polyolefin (fast and uniform) and the short residence time of the volatiles in the reactor. These features help to minimize both the secondary reactions forming aromatics and C_{12+} hydrocarbons and the overcracking to form methane.

The HZSM-5 zeolite catalyst, with a ratio of $SiO_2/Al_2O_3 = 30$, prepared by agglomerating the zeolite with bentonite and alumina and subsequently calcining at 575 °C, has a high activity, which above 450 °C allows for completely transforming the polyolefins into C_{20-} hydrocarbons. The low deactivation of this catalyst is noteworthy, given that it may operate for more than 16 h (1 kg of polyolefin fed into a bed of 30 g of catalyst).

The increase in temperature in the 450−570 °C range leads to a decrease in the yields of C_2-C_4 olefins and nonaromatic components in the C_5-C_{11} fraction, whereas there is an increase in the yields of single-ring aromatics in this fraction. To avoid the operational problems observed at temperatures below 450 °C, which are associated with the presence of waxes in the reaction medium, operation should be carried out at 500 °C. Operation at this temperature is carried out with a space velocity of 2 (g of HDPE) (g of catalyst)$^{-1}$ h^{-1}, four times greater if it is expressed by the mass unit of zeolite; the yields for C_2-C_4 olefins, nonaromatic fraction, single-ring aromatics, and C_{4-} alkanes are 60, 15, 10, and 14 wt %, respectively.

The flow rate of HDPE can even be doubled, and the yields differ only slightly. At 500 °C, the yield of C_2-C_4 olefins decreases slightly (from 58 wt % for 1.0 g min^{-1} to 54 wt % for 2.0 g min^{-1}), with propylene being the one more affected, and the yields of single-ring aromatics and light alkanes increase slightly.

The yields are very similar for the different polyolefins (HDPE, LDPE, and PP), albeit lower for olefins (due to a lower yield of propylene and butenes) and higher for light alkanes and aromatics when LDPE is in the feed. The small difference in the results shows that the technology based on the conical spouted bed reactor with an HZSM-5 zeolite catalyst is suitable for the pyrolysis of different polyolefins.

■ AUTHOR INFORMATION

Corresponding Author

*Tel.: (+34) 946 015414. Fax: (+34) 946 013500. E-mail: gorka. elordi@ehu.es.

■ ACKNOWLEDGMENT

■ REFERENCES

(1) Aguado, J.; Serrano, D. P. *Feedstock Recycling of Plastic Wastes*; The Royal Society of Chemistry: Cambridge, U.K., 1999.

(2) Scheirs, J.; Kaminsky, W. *Feedstock Recycling and Pyrolysis of Waste Plastics, Converting Waste Plastics into Diesel and Other Fuels*; John Wiley and Sons: Chichester, U.K., 2006.

(3) Al-Salem, A. M.; Lettieri, I.; Baeyens, J. Recycling and Recovery Routes of Plastic Solid Waste (PSW): A Review. *Waste Manage.* **2009**, 29, 2625–2643.

(4) Van Grieken, R.; Serrano, D. P.; Aguado, J.; García, R.; Rojo, C. Thermal and Catalytic Cracking of Polyethylene under Mild Conditions. *J. Anal. Appl. Pyrolysis* **2001**, 58−59, 127–142.

(5) Seo, Y.; Lee, K.; Shin, D. Investigation of Catalytic Degradation of High-Density Polyethylene by Hydrocarbon Group Type Analysis. *J. Anal. Appl. Pyrolysis* **2003**, 70, 383–398.

(6) Miskolczi, N.; Bartha, L.; Deák, G.; Jóver, B.; Kalló, D. Thermal and Thermo-catalytic Degradation of High-Density Polyethylene Waste. *J. Anal. Appl. Pyrolysis* **2004**, 72, 235–242.

(7) Cardona, S. C.; Corma, A. Kinetic Study of the Catalytic Cracking of Polypropylene in a Semibatch Stirred Reactor. *Catal. Today* **2002**, 75, 239–246.

(8) Akpanudoh, N. S.; Gobin, K.; Manos, G. Catalytic Degradation of Plastic Waste to Liquid Fuel over Commercial Cracking Catalysts: Effect of Polymer to Catalyst Ratio/acidity Content. *J. Mol. Catal. A: Chem.* **2005**, 235, 67–73.

(9) Achilias, D. S.; Roupakias, C.; Megalokonomos, P.; Lappas, A. A.; Antonakou, E. V. Chemical Recycling of Plastic Wastes Made from Polyethylene (LDPE and HDPE) and Polypropylene (PP). *J. Hazard. Mater.* **2007**, 149, 536–542.

(10) Serrano, D. P.; Aguado, J.; Escola, J. M.; Garagorri, E. Performance of a Continuous Screw Kiln Reactor for the Thermal and Catalytic Conversion of Polyethylene−Lubricating Oil Base Mixtures. *Appl. Catal., B* **2003**, 44, 95–105.

(11) Serrano, D. P.; Aguado, J.; Escola, J. M.; Garagorri, E.; Rodríguez, J. M.; Morselli, L.; Palazzi, G.; Orsi, R. Feedstock Recycling of Agriculture Plastic Film Wastes by Catalytic Cracking. *Appl. Catal., B* **2004**, 49, 257–265.

(12) Mastral, J. F.; Berrueco, C.; Gea, M.; Ceamanos, J. Catalytic Degradation of High Density Polyethylene over Nanocrystalline HZSM-5 Zeolite. *Polym. Degrad. Stab.* **2006**, 91, 3330–3338.

(13) Hernández, M. R.; García, A. N.; Marcilla, A. Catalytic Flash Pyrolysis of HDPE in a Fluidized Bed Reactor for Recovery of Fuel-like Hydrocarbons. *J. Anal. Appl. Pyrolysis* **2007**, 78, 272–281.

(14) Aguado, R.; Olazar, M.; Gaisán, B.; Prieto, R.; Bilbao, J. Kinetic Study of Polyolefins Pyrolysis in a Conical Spouted Bed Reactor. *Ind. Eng. Chem. Res.* **2002**, 41, 4559–4566.

(15) Aguado, R.; Olazar, M.; San José, M. J.; Gaisán, B.; Bilbao, J. Wax Formation in the Pyrolysis of Polyolefins in a Conical Spouted Bed Reactor. *Energy Fuels* **2002**, 16, 1429–1437.

(16) Olazar, M.; San José, M. J.; Peñas, F. J.; Aguayo, A. T.; Bilbao, J. The Stability and Hydrodynamics of Conical Spouted Beds with Binary Mixtures. *Ind. Eng. Chem. Res.* **1993**, 32, 2826–2834.

(17) San José, M. J.; Olazar, M.; Peñas, F. J.; Bilbao, J. Segregation in Conical Spouted Beds with Binary and Tertiary Mixtures of Equidensity Spherical Particles. *Ind. Eng. Chem. Res.* **1994**, 33, 1838–1844.

(18) Altzibar, H.; Lopez, G.; Aguado, R.; Alvarez, S.; San José, M. J.; Olazar, M. Hydrodynamics of Conical Spouted Beds Using Different Types of Internal Devices. *Chem. Eng. Technol.* **2009**, 32, 463–469.

(19) San José, M. J.; Olazar, M.; Peñas, F. J.; Arandes, J. M.; Bilbao, J. Correlation for Calculation of the Gas Dispersion Coefficient in Conical Spouted Beds. *Chem. Eng. Sci.* **1995**, 50, 2161–2172.

(20) Elordi, G.; Olazar, M.; Aguado, R.; Lopez, G.; Arabiourrutia, M.; Bilbao, J. Catalytic Pyrolysis of High Density Polyethylene in a Conical Spouted Bed Reactor. *J. Anal. Appl. Pyrolysis* **2007**, 79, 450–455.

(21) Elordi, G.; Olazar, M.; Lopez, G.; Amutio, M.; Artetxe, M.; Aguado, R.; Bilbao, J. Catalytic Pyrolysis of HDPE in Continuous Mode over Zeolite Catalysts in a Conical Spouted Bed Reactor. *J. Anal. Appl. Pyrolysis* **2009**, 85, 345–351.

(22) Elordi, G.; Olazar, M.; Lopez, G.; Artetxe, M.; Bilbao, J. Product Yields and Compositions in the Continuous Pyrolysis of High Density Polyethylene in a Conical Spouted Bed Reactor. *Ind. Eng. Chem. Res.* **2011**, doi: 10.1021/ie200186m.

(23) Ali, S.; Garforth, A. A.; Harris, D. H.; Rawlence, D. J.; Uemichi, Y. Polymer Waste Recycling over "Used" Catalysts. *Catal. Today* **2002**, 75, 247–255.

(24) Hernández, M. R.; García, A. N.; Marcilla, A. Study of the Gases Obtained in Thermal and Catalytic Flash Pyrolysis of HDPE in a Fluidized Bed Reactor. *J. Anal. Appl. Pyrolysis* **2005**, 73, 314–322.

(25) Lin, Y. H.; Yang, M. H. Catalytic Reactions of Post-Consumer Polymer Waste over Fluidised Cracking Catalyst for Producing Hydrocarbons. *J. Mol. Catal. A: Chemical* **2005**, 231, 113–122.

(26) Lin, Y. H.; Yen, H. Y. Fluidised Bed Pyrolysis of Polypropylene over Cracking Catalysts for Producing Hydrocarbons. *Polym. Degrad. Stab.* **2005**, 89, 101–108.

(27) Marcilla, A.; Beltrán, M. I.; Navarro, R. Study of the Deactivation Process of HZSM5 Zeolite during Polyethylene Pyrolysis. *Appl. Catal., A* **2007**, 333, 57–66.

(28) Marcilla, A.; Gómez-Siurana, A.; Berenguer, D. Study of the Decomposition of Low Density Polyethylene Blends with Vacuum Gas Oils: Evolution of the Gases. *Polym. Degrad. Stab.* **2008**, 93, 2204–2213.

(29) Marcilla, A.; Gómez-Siurana, A.; Valdés, F. J. Influence of the Temperature on the Composition of the Coke Obtained in the Catalytic Cracking of Low Density Polyethylene in the Presence of USY and HZSM-5 Zeolites. *Microporous Mesoporous Mater.* **2008**, 109, 420–428.

(30) Marcilla, A.; Gómez-Siurana, A.; Valdés, F. J. Evolution of the Deactivation Mode and Nature of Coke of HZSM-5 and USY Zeolites in the Catalytic Cracking of Low-density Polyethylene During Successive Cracking Runs. *Appl. Catal., A* **2009**, 352 (2009), 152–158.

(31) Boronat, M.; Corma, A. Are Carbenium and Carbonium Ions Reaction Intermediates in Zeolite-Catalyzed Reactions? *Appl Catal., A* **2008**, 336, 2–10.

(32) Elordi, G.; Olazar, M.; Lopez, G.; Castaño, P.; Bilbao, J. Role of Pore Structure in the Deactivation of Zeolites (HZSM-5; Hβ and HY) by Coke in the Pyrolysis of Polyethylene. *Appl. Catal., B* **2011**, 102, 224–231.

(33) Valle, B.; Gayubo, A. G.; Alonso, A.; Aguayo, A. T.; Bilbao, J. Hydrothermally Stable HZSM-5 Zeolite Catalysts for the Transformation of Crude Bio-oil into Hydrocarbons. *Appl. Catal., B* **2010**, 100, 318–327.

(34) Guisnet, M.; Magnoux, P. Organic Chemistry of Coke Formation. *Appl. Catal., A* **2001**, 212, 83–96.

6069

dx.doi.org/10.1021/ie2002999 |*Ind. Eng. Chem. Res.* 2011, 50, 6061–6070

(35) Cerqueira, H. S.; Caeiro, G.; Costa, L.; Ramôa Ribeiro, F. Deactivation of FCC Catalysts. *J. Mol. Catal. A: Chem.* **2008**, *292*, 1–13.

(36) Guisnet, M.; Costa, L.; Ramôa Ribeiro, F. Prevention of Zeolite Deactivation by Coking. *J. Mol. Catal. A: Chem.* **2009**, *305*, 69–83.

(37) Olazar, M.; San José, M. J.; Aguayo, A. T.; Arandes, J. M.; Bilbao, J. Stable Operation Conditions for Gas—Solid Contact Regimes in Conical Spouted Beds. *Ind. Eng. Chem. Res.* **1992**, *31*, 1784–1791.

(38) Olazar, M.; San José, M. J.; Aguayo, A. T.; Arandes, J. M.; Bilbao, J. Design Factors of Conical Spouted Beds and Jet Spouted Beds. *Ind. Eng. Chem. Res.* **1993**, *32*, 1245–1250.

(39) Olazar, M.; San José, M. J.; Alvarez, S.; Morales, A.; Bilbao, J. Measurement of Particle Velocities in Conical Spouted Beds Using an Optical Fiber Probe. *Ind. Eng. Chem. Res.* **1998**, *37*, 4520–4527.

(40) Olazar, M.; San José, M. J.; Alvarez, S.; Morales, A.; Bilbao, J. Design of Conical Spouted Beds for the Handling of Low Density Solids. *Ind. Eng. Chem. Res.* **2004**, *43*, 655–661.

(41) San José, M. J.; Olazar, M.; Alvarez, S.; Bilbao, J. Local Bed Voidage in Conical Spouted Beds. *Ind. Eng. Chem. Res.* **1998**, *37*, 2553–2558.

(42) San José, M. J.; Olazar, M.; Alvarez, S.; Izquierdo, M. A.; Bilbao, J. Solid Cross-Flow into the Spout and Particle Trajectories in Conical Spouted Beds. *Chem. Eng. Sci.* **1998**, *53*, 3561–3570.

(43) San José, M. J.; Olazar, M.; Alvarez, S.; Morales, A.; Bilbao, J. Spout and Fountain Geometry in Conical Spouted Beds Consisting of Solids of Varying Density. *Ind. Eng. Chem. Res.* **2005**, *44*, 193–200.

(44) San José, M. J.; Olazar, M.; Alvarez, S.; Morales, A.; Bilbao, J. Local Porosity in Conical Spouted Beds Consisting of Solids of Varying Density. *Chem. Eng. Sci.* **2005**, *60*, 2017–2025.

(45) San José, M. J.; Alvarez, S.; Ortiz de Salazar, A.; Olazar, M.; Bilbao, J. Operating Conditions of Conical Spouted Beds with a Draft Tube. Effect of the Diameter of the Draft Tube and of the Height of Entrainment Zone. *Ind. Eng. Chem. Res.* **2007**, *46*, 2877–2884.

(46) Kim, J.; Choi, M.; Ryoo, R. Effect of Mesoporosity against the Deactivation of MFI Zeolite Catalyst during the Methanol-to-Hydrocarbon Conversion Process. *J. Catal.* **2010**, *269*, 219–228.

(47) Benito, P. L.; Aguayo, A. T.; Gayubo, A. G.; Bilbao, J. Catalyst Equilibration for Transformation of Methanol into Hydrocarbons by Reaction—Regeneration Cycles. *Ind. Eng. Chem. Res.* **1996**, *35*, 2177–2182.

(48) Argauer, R. J.; Landolt, G. R. Crystalline Zeolite HZSM-5 and Method of Preparing the Same. U.S. Patent 3,702,886, 1972.

(49) Olson, D. H.; Kokotailo, G. T.; Lawton, S. L.; Meier, W. M. Crystal-Structure and Structure-Related Properties of ZSM-5. *J. Phys. Chem.* **1981**, *85*, 2238–2243.

(50) Aguayo, A. T.; Gayubo, A. G.; Vivanco, R.; Olazar, M.; Bilbao, J. Role of Acidity and Microporous Structure in Alternative Catalysts for the Transformation of Methanol into Olefins. *Appl. Catal., A* **2005**, *283*, 197–207.

(51) Corma, A.; Huber, G. W.; Sauvanaud, L.; O'Connor, P. Processing Biomass-Derived Oxygenates in the Oil Refinery: Catalytic Cracking (FCC) Reaction Pathways and Role of Catalyst. *J. Catal.* **2007**, *247*, 307–327.

(52) Arandes, J. M.; Abajo, I.; Fernández, I.; Azkoiti, M. J.; Bilbao, J. Effect of HZSM-5 Zeolite Addition to a FCC Catalyst. Study in a Laboratory Reactor Operating under Industrial Conditions. *Ind. Eng. Chem. Res.* **2000**, *39*, 1917–1924.

(53) Buchanan, J. S. The Chemistry of Olefins Production by ZSM-5 Addition to Catalytic Cracking Units. *Catal. Today* **2000**, *55*, 207–212.

(54) Olazar, M.; San José, M. J.; Aguado, R.; Gaisán, B.; Bilbao, J. Bed Voidage in Conical Sawdust Beds in the Transition Regime between Spouting and Jet Spouting. *Ind. Eng. Chem. Res.* **1999**, *38*, 4120–4122.

(55) Elordi, G. Ph.D. Thesis, Thermal and Catalytic Pyrolysis of Polyolefins in a Conical Spouted Bed Reactor, University of the Basque Country, Bilbao, Spain, 2010.

(56) Gayubo, A. G.; Aguayo, A. T.; Castilla, M.; Olazar, M.; Bilbao, J. Consideration of the Role of Water in the Kinetic Modelling of HZSM-5 Zeolite Deactivation by Coke in the Transformation of Methanol into Hydrocarbons. *AIChE J.* **2002**, *48*, 1561–1571.

(57) Gayubo, A. G.; Tarrío, A. M.; Aguayo, A. T.; Olazar, M.; Bilbao, J. Kinetic Modelling of the Transformation of Aqueous Ethanol into Hydrocarbons on a HZSM-5 Zeolite. *Ind. Eng. Chem. Res.* **2001**, *40*, 3467–3474.

(58) Predel, M.; Kaminsky, W. Pyrolysis of Mixed Polyolefins in a Fluidised-Bed Reactor and on a Pyro-GC/MS to Yield Aliphatic Waxes. *Polym. Degrad. Stab.* **2000**, *70*, 373–385.

(59) Encinar, J. M.; González, J. F. Pyrolysis of Synthetic Polymers and Plastic Wastes. Kinetic Study. *Fuel Process. Technol.* **2008**, *89*, 678–686.

(60) Hujuri, U.; Ghoshal, A. K.; Gumma, S. Modeling Pyrolysis Kinetics of Plastic Mixtures. *Polym. Degrad. Stab.* **2008**, *93*, 1832–1837.

(61) Chowlu, A. Ch. K.; Reddy, P. K.; Ghoshal, A. K. Pyrolytic Decomposition and Model-Free Kinetics Analysis of Mixture of Polypropylene (PP) and Low-Density Polyethylene (LDPE). *Thermochim. Acta* **2009**, *485*, 20–25.

(62) Jung, S. H.; Cho, M. H.; Kang, B. S.; Kim, J. S. Pyrolysis of a Fraction of Waste Polypropylene and Polyethylene for the Recovery of BTX Aromatics Using a Fluidized Bed Reactor. *Fuel Process. Technol.* **2010**, *91*, 277–284.

(63) Miskolczi, N.; Bartha, L.; Angyal, A. Pyrolysis of Polyvinyl Chloride (PVC)-Containing Mixed Plastic Wastes for Recovery of Hydrocarbons. *Energy Fuels* **2009**, *23*, 2743–2749.